Dose-dependent phorbol 12-myristate-13-acetate-mediated monocyte-to-macrophage differentiation induces unique proteomic signatures in THP-1 cells

Sneha M. Pinto †, ‡*, Hera Kim †*, Yashwanth Subbannayya †, Miriam Giambelluca †, Korbinian Bösl †° and Richard K. Kandasamy †, §, #

†Centre of Molecular Inflammation Research (CEMIR), and Department of Clinical and Molecular Medicine (IKOM), Norwegian University of Science and Technology, N-7491 Trondheim, Norway

‡Center for Systems Biology and Molecular Medicine, Yenepoya (Deemed to be University), Mangalore, India

°Department of Infectious Diseases, Medical Clinic, St. Olavs Hospital, N-7491 Trondheim, Norway

§Centre for Molecular Medicine Norway (NCMM), Nordic EMBL Partnership, University of Oslo and Oslo University Hospital, N-0349 Oslo, Norway

¶Program in Innate Immunity, Division of Infectious Diseases and Immunology, Department of Medicine, University of Massachusetts Medical School, Worcester, MA, United States

Correspondence: Richard K. Kandasamy (richard.k.kandasamy@ntnu.no)

* These authors contributed equally

Running title: Proteomics of PMA-mediated differentiation of THP-1 cells

Abstract

Macrophages are sentinels of the innate immune system, and the human monocytic cell line THP-1 is one of the widely used *in vitro* models to study immune responses. Several monocyte-to-macrophage differentiation protocols exist, with phorbol 12-myristate-13-acetate (PMA) being the widely used and accepted method. However, the concentrations and duration of PMA treatment vary widely in the published literature and their effect on protein expression is not fully deciphered. In this study, we employed a dimethyl labeling-based quantitative proteomics approach to determine the changes in the protein repertoire of macrophage-like cells differentiated from THP-1 monocytes by three commonly used PMA-based differentiation protocols. Our analysis shows that variations in PMA concentration and duration of rest post-stimulation result in downstream differences in the protein expression and cellular processes. We demonstrate that these differences result in altered gene expression of cytokines upon stimulation with various TLR agonists. Together, these findings provide a valuable resource that significantly expands the knowledge of protein expression dynamics with one of the most common *in vitro* models for macrophages, which in turn has a profound impact on the immune responses being studied.

Keywords: Monocyte, Macrophage, TLR signaling, innate immune signaling, pathway analysis, functional networks, pathways, differentiation, quantitative proteomics.

Introduction

Macrophages and their precursors- monocytes, mediate innate immune responses and inflammatory processes, and also contribute to adaptive immunity through antigen presentation (1, 2). Monocytes in the blood circulation migrate to the site of infection/inflammation and differentiate into macrophages for effective host defense, tissue remodeling, and repair (3). Furthermore, macrophages exhibit a high level of plasticity, depending on their local microenvironment, specialized functions and varied phenotype acquired (1, 4).

Several models are employed to study the mechanisms of immune-modulation in monocytes and macrophages during inflammatory diseases. The most frequently used include primary peripheral blood mononuclear cells (PBMCs) and monocyte cell lines. However, due to donor-to-donor variations and technical disparities involved in handling of PBMCs *in vitro*, the human leukemia monocytic cell line, THP-1, is widely accepted and used as a monocyte/macrophage model (5, 6). Several studies have indicated that THP-1 cells can be differentiated into macrophage-like cells using phorbol-12-myristate-13- acetate (PMA), which markedly resembles PBMC monocyte-derived macrophages (MDMs) in cytokine production, metabolic and morphological properties, including differential expression of macrophage surface markers such as *CD14*, CD11b (*ITGAM*) and scavenger receptors- *CD163*, *MSR1*, and *SCARB2* (5, 7-10). Nonetheless, depending on the parameters of the differentiation protocol employed, such as the concentration (ranging from 5 to 400 ng/mL), and duration of incubation (1 to 5 days) with PMA; the degree of differentiation and the functional changes may vary significantly (5, 11-15).

At the molecular level, multiple proteins including growth factors, antigenic markers, chemokine-receptors, cytokines, and cell adhesion molecules, are known to govern and reflect underlying monocyte-macrophage differentiation processes (16-20). However, the effect of various differentiation protocols on the cellular proteome and intracellular signaling networks

during monocyte-to-macrophage differentiation remains poorly understood. Hence, it is crucial to determine the most suitable differentiation conditions when using these cells as model system, as this can significantly impact their response to various innate immune stimuli. Quantitative high-resolution mass spectrometry-based proteomic approaches have been widely employed to investigate the proteomes of monocytes and macrophages as well as altered cellular proteomes and complex cellular/biological mechanisms in several biological conditions (21-23). However, to date, no studies have directly compared the proteome changes of the PMA-mediated differentiation process.

In the present study, we evaluate the effect of three PMA-based differentiation protocols on the changes in the proteome profiles upon THP-1 differentiation using stable isotope dimethyl labeling quantitative proteomics. We demonstrate that various differentiation conditions such as concentration and incubation time, prior to any stimuli, are critical consideration factors for heterogeneity of the cell culture. The results from this study will enable immunologists to make informed decisions on differentiation protocols that result in the desired proteotypes for custom experiments.

Material and methods

Cell culture and differentiation

Human THP-1 monocytic cells (ATCC) were cultured in RPMI 1640 (Sigma-Aldrich) medium containing 10% heat-activated fetal calf serum (FCS), 2 mM L-glutamine, 100 nM penicillin/streptomycin (Thermo Fisher Scientific) and 50 μM β-mercaptoethanol (Sigma-Aldrich). The cells were maintained in a humidified 37°C, 5% CO_2 incubator. THP-1 cells were differentiated into resting macrophages by resuspending the cells in growth medium containing 5 or 50 ng/ml phorbol-12-myristate-13-acetate (PMA; Sigma-Aldrich) and cultured for indicated time periods. The process of differentiation was enhanced by removing the PMA-containing media and adding fresh, complete RPMI 1640 media to the cells. The treatment conditions included the following. **Condition A**: 50 ng/ml PMA for 72 hours followed by 48 hours rest (5 days); **Condition B**: 50 ng/ml PMA overnight (16 hours) followed by 48 hours rest (Condition B); and **Condition C**: 5 ng/ml PMA for 48 hours followed by 3 hours rest (5, 11-14).

Phase-contrast microscopy

THP-1 cells were seeded at a density of 0.2 x 10^6 cells/ml in cell culture Cellvis glass-bottom plates and treated with PMA and rested at indicated concentrations and duration. The morphological characteristics of undifferentiated and differentiated THP-1 cells were captured by EVOS FL Auto Cell Imaging System 2 (Thermo Fisher Scientific) using a 40x objective lens and were processed by ImageJ software (W.S. Rasband, National Institutes of Health, Bethesda, MD).

Flow cytometry

THP-1 cells were plated in 12-well culture plates (Corning Costar) as described above. The cells were washed three times with 1X PBS and detached from plates using Accutase (A6964; Sigma-Aldrich) incubation for 15 minutes at 37℃. The detached cells were collected on ice

and then centrifuged (settings). Human TruSatin FcX™, FcR Blocking Reagent (1 µg IgG/10^6 cells in 100 µl staining volume; BioLegend, #422301) was applied to decrease the non-specific binding for 10 minutes on ice. Cells were subsequently stained with Brilliant Violet 785™ anti-human CD14 Antibody (1:1000; BioLegend, #301840), APC anti-human CD86 Antibody (1:1000; BioLegend, #305412), and PE anti-human CD11b Antibody (1:1000; BioLegend, #301306) for 30 minutes in the dark. The cells were then fixed and permeabilized with 1% paraformaldehyde (PFA). Flow cytometry data were acquired on a BD LSRII flow cytometer (BD Biosciences) with FACS Diva software (BD) and analyzed using FlowJo software (FlowJo, LLC).

Cell lysis and sample preparation for mass spectrometry

The cells for proteomic analysis were cultured, as described above. After the indicated time points of PMA incubation followed by resting, the media was discarded, and the cells were washed thrice with ice cold PBS. The cells were lysed, and harvested using SDS lysis buffer (2% SDS in 50 mM TEABC) tubes and sonicated using a probe sonicator (Branson Digital Sonifier) on ice for 5-10 minutes (20% amplitude, 10 cycles). The lysates were heated at 95ºC for 10 minutes, allowed to cool to room temperature, and centrifuged at 12,000 rpm for 10 minutes. The protein concentration in the lysates were estimated by the Bicinchoninic acid (BCA) assay (Pierce, Waltham, MA). 200 µg proteins from each condition were reduced and alkylated with dithiothreitol (DTT) at 60°C for 20 minutes and 20 mM iodoacetamide (IAA) at room temperature for 10 minutes in the dark, respectively. The protein samples were then subjected to acetone precipitation with five volumes of chilled acetone at -20ºC for 6 hours. Protein pellets were obtained by centrifugation at 12,000 rpm for 15 minutes at 4 ºC and subjected to trypsin digestion with sequencing grade trypsin (1:20) (Sigma Aldrich) overnight at 37 ºC.

Dimethyl-labeling of tryptic peptides

The tryptic peptides obtained from Condition A, B and C were subjected to reductive dimethylation with 4% (vol/vol) formaldehyde (CH_2O) (Light), (CD_2O) (Medium) or ($^{13}CD_2O$) (Heavy) labels respectively. Following this, 4 µl of 0.6 M sodium cyanoborohydride ($NaBH_3CN$) was added to the samples to be labeled with light and intermediate labels and 4 µl of 0.6 M sodium cyanoborodeuteride ($NaBD_3CN$) to the sample to be heavy labeled respectively. The mixture was incubated for 1 hour at room temperature. The reaction was quenched with 16 µl of 1% ammonia. Finally, 8 µl formic acid was added, and the three differentially labeled samples were pooled and desalted using C_{18} StageTip, evaporated to dryness under vacuum, and subjected to Stage-tip based Strong-cation exchange (SCX) fractionation as described previously (24).

Mass spectrometry analysis

Mass spectrometric analyses of the SCX fractions were carried out using a Q Exactive HF Hybrid Quadrupole-Orbitrap mass spectrometer (Thermo Fisher Scientific, Bremen, Germany) coupled to Easy-nLC1200 nano-flow UHPLC (Thermo Scientific, Odense, Denmark). The data were acquired for each of the samples in biological quadruplicates. Briefly, tryptic peptides obtained from StageTip-based SCX fractionation were reconstituted in 0.1% formic acid and loaded on a nanoViper 2 cm (3 µm C18 Aq) trap column (Thermo Fisher Scientific). Peptide separation was carried out using EASY-Spray C18 analytical column (50 cm, 75µm PepMap C18, 2 µm C18 Aq) (ES801, Thermo Fisher Scientific) set at 40°C. Peptide separation was carried out at a flow rate of 250 nl/min using a binary solvent system containing solvent A: 0.1% formic acid and solvent B: 0.1% formic acid in 80% acetonitrile. A linear gradient of 5-30% solvent B over 150 minutes, followed by a linear gradient of 30-95% solvent B for 5 minutes, was employed to resolve the peptides. The column was re-equilibrated to 5% solvent B for an additional 20 minutes. The total run time was 180 minutes. Data were acquired in positive mode using a data-dependent acquisition method wherein MS1 survey scans were

carried out in 350-1650 m/z range in Orbitrap mass analyzer at a mass resolution of 120,000 mass resolution at 200 m/z. Peptide charge state was set to 2-6, and dynamic exclusion was set to 30 s along with an exclusion width of ± 20 ppm. MS/MS fragmentation was carried out for the most intense precursor ions selected at top speed data-dependent mode with the maximum cycle time of 3 seconds HCD fragmentation mode was employed with a collision energy of 30% and detected at a mass resolution 15,000 at m/z 200. Internal calibration was carried out using a lock mass option (m/z 445.1200025) from ambient air.

Data analysis

Protein identification and quantification were performed using Proteome Discoverer Version 2.3 with the following parameters: carbamidomethyl of cysteine as a fixed modification, and oxidation of methionine, deamidation of asparagine and glutamine, acetylation (protein N terminus), quantitation labels Dimethyl, Dimethyl:2H4 and Dimethyl:2H(6)13C(2) on N-terminal and/or lysine were set as variable modifications. Trypsin as specified as proteolytic enzyme with maximum of 2 missed cleavages allowed. The searches were conducted using the SequestHT node against the Uniprot-Trembl Human database (v2017-10-25), including common contaminants. Mass accuracy was set to 10 ppm for precursor ions and 0.02 Da for MS/MS data. Identifications were filtered at a 1% false-discovery rate (FDR), accepting a minimum peptide length of 7 amino acids. Quantification of identified proteins referred to the razor and unique peptides and required a minimum ratio count of 2. Dimethyl-based relative ratios were extracted for each protein/condition using the Minora Feature Detector node and were used for downstream analyses.

Bioinformatics analysis

Protein abundances across multiple replicates were scaled, log-transformed, normalized using the cyclic loess method, and analyzed for differential expression in limma v3.38.3 (25) in R/Bioconductor (v3.5.2, https://www.r-project.org/; v3.8 https://bioconductor.org). The

treatment conditions were used for contrasting . Proteins expressed with a log2-fold change ≥±2 were considered as differentially expressed. Volcano plots were drawn using the EnhancedVolcano R package (v 1.0.1) and proteins with –log10 (p-value) ≥ 1.25 were considered to be significant. Heatmaps of expression data and *k*-means clustering was carried out in Morpheus using Euclidean complete linkage (https://software.broadinstitute.org/morpheus/). Significant clusters of genes that were overexpressed in conditions A, B, and C were extracted, and enriched biological processes were identified using Enrichr (https://amp.pharm.mssm.edu/Enrichr/). Hypergeometric enrichment-based pathway analysis was carried out using ReactomePA (1.28.0) in R (v3.6.0, https://www.r-project.org/)/Bioconductor (v3.9 https://bioconductor.org) with clusterProfiler 3.12.0 (26). Genesets with a minimum of 15 genes were considered for the analysis. The plot was visualized using the ggplot2 package (v3.2.1) (https://cran.r-project.org/web/packages/ggplot2). Significantly changing clusters for each condition from the *k*-means clustering analysis were subjected to network analysis using STRING in Cytoscape (version 3.7.1). The network properties were calculated using NetworkAnalyzer and visualized in Cytoscape using betweenness centrality and degree parameters. The entire networks were further subjected to clustering to identify significant sub-clusters using the MCODE app (v1.5.1) (27) in Cytoscape. The parameters used for clustering included degree cutoff of 2, node score cutoff of 0.2, *k*-core of 2, and Max. Depth of 100. Kinome trees were drawn using KinMap (28) (http://kinhub.org/kinmap). Gene lists for functions such as phagocytosis, reactive oxygen species, and inflammasome complex were obtained from the Molecular Signatures Database (MSigDB, v7.0, https://www.gsea-msigdb.org/gsea/msigdb) (29). Protein kinase and phosphatase lists were obtained from previous studies (30-33)

Western blot analysis

Protein samples were run on pre-cast NuPAGE™ Bis-Tris gels (Invitrogen) with 1 x MOPS buffer (Invitrogen) and transferred on nitrocellulose membranes, using the iBlot®2 Gel Transfer Device (Invitrogen). Membranes were washed in Tris Buffered Saline with 0.1% Tween-X100 (TBS-T) and blocked with TBS-T containing 5% bovine serum albumin (BSA, Sigma-Aldrich). Membranes were incubated with primary antibodies at 4°C overnight. The following primary antibodies were used: GAPDH (1:5000; ab8245; Abcam), anti-IRF3 (1:1000; D83B9; cat#4302S; Abcam), anti-TBK1 (1:1000; cat#3504; Cell Signaling Technology), anti- IL1B (1:1000; cat#12242; Cell Signaling Technology) and SQSTM1 (1:1000; cat#PM045; MBL). Membranes were washed in TBS-T and incubated with secondary antibodies (HRP-conjugated, DAKO) for 1 hour at room temperature in TBS-T containing 1% milk or BSA, developed with SuperSignal West Femto Substrate (Thermo Scientific) and captured with LI-COR Odyssey system (LI-COR Biosciences, Lincoln, NE, USA).

RNA isolation and quantitative real-time PCR (qPCR) analysis

Undifferentiated THP-1 and PMA-differentiated cells (2 x 10^5 cells) in biological duplicates per condition were stimulated with TLR agonists- CL075 (TLR8; tlrl-c75; Invivogen, 5 µg/ml), CpG2006 (TLR9; tlrl-2006; Invivogen, 10 µM), Flagellin (TLR5; tlrl-stfla; Invivogen, 100 ng/ml), FSL1 (TLR2/6; tlrl-fsl; Invivogen, 100 ng/ml), LPS 0111:B4 (TLR4; tlrl-3pelps; Invivogen, 200 ng/ml), LPS K12 (TLR4; tlrl-eklps; Invivogen, 200 ng/ml), Pam3CSK4 (TLR1/2; tlrl-pms; Invivogen, 200 ng/ml), Poly (I:C) (TLR3; vac-pic; Invivogen, 10 µg /ml), R837 (TLR7; tlrl-imqs; Invivogen, 10 µg/ml), and R848 (TLR7/8; tlrl-r848; Invivogen, 100 ng/ml) for 4 hours. Post stimulation, total RNA was isolated using RNeasy Mini columns, followed by DNAse digestion (Qiagen), according to the manufacturer's protocol. The purity and concentrations of RNA were determined using NanoDrop 1000 (Thermo Scientific). cDNA was prepared with High-Capacity RNA-to-cDNA™ (Applied Biosystems). Quantitative real-time PCR (qPCR) analysis was performed on StepOne Plus Real-Time PCR

cycler (Thermo Fisher Scientific) using PerfeCTa qPCR FastMix UNG (Quantabio) and FAM Taqman Gene Expression Assays: *IL6* Hs00985639_m1, *IL1B* Hs00174097_m1, *TNF* Hs01113624_g1, *TBP* Hs00427620_m1, *IL8* Hs00174103_m1 (Life Technologies) in 96-well format in technical duplicates. Relative expression compared to the unstimulated control samples and TBP as a house keeping gene was calculated in R 3.3.2 as described previously (25).

Data availability

Mass spectrometry-derived data have been deposited to the ProteomeXchange Consortium (http://proteomecentral.proteomexchange.org) via the PRIDE partner repository (26) with the dataset identifier: PXD015872.

Results

PMA differentiation induces changes in morphology and expression of cell surface markers in THP-1 cells

We aimed to investigate the effects of various concentrations and duration of incubation with PMA on the differentiation of THP-1 monocytic cells to macrophage-like cells. We chose three commonly used differentiation protocols for the analysis based on previous studies (7, 12, 27). Light microscopy analysis revealed changes in PMA induced morphology, including increased cellular adhesion and spread morphology. In concordance with the results observed by Starr *et al.* (28), the changes in cell morphology were dependent on the concentration and the duration of incubation, with cells treated with PMA and rested for two days showing a significant increase in cytoplasmic volume with increased adherence (**Figure 1A**). The differentiation was more pronounced in Condition A in comparison with the conditions B and C. Additionally, flow cytometry analyses indicated an increase in side scatter (SSC), in condition A with respect to conditions B and C. The cells treated with PMA but not rested (Condition C) closely resembled the undifferentiated THP-1 cells in regard to these properties (**Figure 1B**). In addition to the morphological changes, the differential expression of cell surface markers CD86, CD11b (ITGAM), and CD14 were also monitored. CD86, a cell surface glycoprotein expressed on all antigen-presenting cells, was found to be expressed to a similar extent in all the three protocols tested. In concordance with earlier reports, the expressions of CD11b and CD14 were found to be lower in Condition C in comparison to the other two conditions tested. We also observed an effect on the expression based on the duration of incubation and period of rest. The expression of both CD11b and CD14 was comparable in conditions A and B with the highest surface expression observed in condition A (**Figure 1C**). Our data, therefore, confirm the previous findings that the degree of differentiation induced by PMA treatment varies depending on the concentration and period of rest post-PMA treatment.

Quantitative proteomic analysis reveals diverse proteome expression profiles in response to varying differentiation protocols

To evaluate the proteome-wide expression changes upon PMA treatment, we performed quantitative proteomic analysis using a stable isotope dimethyl labeling approach (**Figure 2A**). From four independent biological replicates, 5,277 proteins were identified, of which 5,006 proteins were quantified in at least one replicate. A total of 3,623 proteins were identified and quantified in all four replicates providing a global view of changes in protein expression upon PMA treatment (**Supplementary Table 1**). Principal component analysis (PCA) revealed distinct clustering of each treatment condition with the biological replicates grouped (**Figure 2B**). The highest variance was observed in all replicates of condition C and can likely be explained by the fact that the morphological phenotype observed was much closer to the monocytic cell type rather than the macrophage-like phenotype.

Next, we applied a log2 (fold-change) and adjusted p-value cutoff of 2 and < 0.05 resulting in the identification of 324, 415 and 413 proteins upregulated and 299, 321 and 338 proteins downregulated in condition B with respect to condition A (B/A), condition C with respect to condition A (C/A) and condition B (C/B), respectively (**Figure 2 C-E, Supplementary Figure 1A**). The segregation of condition A from condition B and C was mainly driven by differential expression of several proteins involved in vesicle-mediated transport (KIF13B, KIF2C, KIFC1, STX18), cell cycle regulation and mitosis (RRM1 and RRM2), DNA polymerase complex subunits- POLD1 and POLD2, topoisomerase TOP2A, TACC3, and PRKACB. Interestingly, proteins involved in innate immune response such as TBK1, IRF3, IL1B, scavenger receptor SCARB1, and mitochondrial translation initiation factor MTIF3 were significantly differentially expressed in condition B in comparison to conditions A and C. On the contrary, members of the aldehyde dehydrogenase family such as ALDH1L2, ALDH2, members of serine/threonine-protein kinase C (PRKCA, PRKCB, PRKCD), proteins involved in amino

acid metabolism-GOT1, PSAT1, ASNS among others were found to be significantly upregulated in condition C in comparison to conditions A and B. It has been previously shown that PMA-mediated differentiation increases the expression of PKC isoenzymes albeit to a varied extent (29). The results from the MS analysis were further confirmed by validating the expression dynamics of select proteins using immunoblot analysis. Consistent with MS results, the expression of IRF3, TBK1, IL1B, and SQSTM1 were upregulated in cells differentiated for 3 and 5 days (**Supplementary Figure 1B**).

Monocyte-to-macrophage differentiation is reportedly associated with changes in the expression of cell surface proteins, and this phenomenon has been utilized to distinguish macrophage subtypes by their pattern of cell surface receptor expression (7, 30). Our analysis revealed increased expression of known macrophage cell-surface markers such as TFRC (CD71), FCGR1B, scavenger receptors- CD163, MSR1, and SCARB2 mainly in conditions A and B. Notably, CD163, a member of the scavenger receptor cysteine-rich (SRCR) superfamily class B, has been previously reported to be highly expressed in macrophages with low expression reported in monocytes, dendritic cells and Langerhans cells (31, 32). On the contrary, the expression of CD68 and CD14 in agreement with previous studies were downregulated in condition B, suggesting a phenotype closer to macrophages. Interestingly, the expression of CD36 and ITGAM (CD11b) was upregulated in condition A with respect to conditions B and C, whereas that of CD68 was downregulated in both conditions A and B with respect to condition C (**Supplementary Figure 1C, Table 1**). Comparison with the known macrophage differentiation markers (GO:0030225) revealed significant induction of CSF1R, TLR2, APP, RB1, CASP8, FADD, MMP9 and ICAM1 in conditions A and B with the exception of transcription factor PU.1 (SPI1) and PRKCA that were significantly up in condition C and CDC42 that was expressed to similar extent in all three protocols tested.

Cluster analysis reveals differentiation protocol-specific regulation of cellular processes and signaling pathways

To gain further insights into specific expression profiles, we performed unsupervised hierarchical clustering of proteins quantified, which revealed a high correlation between biological replicates. Using Euclidean average and k-means clustering, the differentially expressed genes were segregated into 10 major clusters (**Figure 3A, Supplementary Table 2**). Cluster 1, 7, and 10 included proteins upregulated in conditions B, A, and C, respectively. Cluster 3 includes 290 proteins that were expressed to a similar extent in conditions B and C but downregulated in condition A. On the contrary; Cluster 6 included 458 proteins that were expressed to a similar extent in conditions A and B but downregulated in condition C and cluster 9 comprised of proteins overexpressed in conditions A and C with respect to condition B, but with an overall increased expression observed in all replicates of condition C. Clusters 2, 4 and 5 showed similar expression of proteins across all three protocols tested with varying expression across replicates. Altogether, our analysis demonstrates the existence of common and differentiation-protocol-specific proteome signatures.

Gene ontology analysis of the differentiation protocol-specific clusters (clusters 1, 7, and 10) revealed significant enrichment of several biological processes (adjusted p-value < 0.05) (**Figure 3B, Supplementary Table 3-5**). Across the three differentiation conditions, several metabolic processes were enriched. Processes indicative of differentiation, such as cell migration and mitotic nuclear envelope assembly, were also enriched. While immune response-regulating cell surface receptor signaling pathway was observed to be primarily enriched in condition B, the process of leukocyte mediated immunity was found to be enriched in conditions A and C (**Supplementary Figure 2**). Regulation of translation and gene expression were among the significantly enriched processes in Cluster 3 and 6, whereas in the case of Cluster 9, which included proteins expressed to a similar extent in conditions A and C but

downregulated in condition B, we observed enrichment of carbohydrate and fatty acid metabolic processes. (**Supplementary Figure 2**). The findings described above are consistent with the morphological changes observed with processes indicative of differentiation, such as cell migration, gene expression, ribosome biogenesis as well as that of immune cell function which were largely enriched in conditions A and B respectively.

Pathway enrichment and network analysis reveals kinases as key regulatory hubs of the PMA mediated differentiation processes

We next aimed to delineate the signaling pathways affected during monocyte-to-macrophage differentiation. Pathway enrichment analysis using the Reactome database revealed differentiation protocols specific enrichment of signaling pathways such as VEGF signaling pathway (enriched in conditions A and B), metabolism of nucleotides and porphyrins (enriched in condition A), Fc epsilon R1 signaling (enriched in condition B), activation of NADPH oxidases by RhoGTPases, and glycosphingolipid metabolism (enriched specifically in condition C) (**Figure 4A, Supplementary Table 6**). Interestingly, cell surface signaling mediated by ephrins, integrin, semaphorin, and syndecan interactions were significantly enriched in condition A with respect to condition C with no apparent differences observed with condition B. On the contrary, signaling pathways involved in clearing infections and immune responses were significantly enriched in condition B. Apoptotic pathways were found to be downregulated, whereas transamination and amino acid synthesis were upregulated in condition C.

Network analyses of k-means clusters upregulated in each condition **(Supplementary Figure 3-5, Supplementary Table 7)** enabled identification of distinct hub proteins. Interestingly, several kinases involved in cellular processes namely cell proliferation, differentiation and regulation of microtubule dynamics such as MAPK1, CDK1, and PRKACB were found to have a high degree of betweenness centrality and exist as key regulatory hubs in the network for

condition A. Other key regulatory hubs included DUT, FN1 a glycoprotein involved in cell adhesion and migration processes and SEC13, a core component of the COPII-coated vesicles and nuclear core complex . While proteins involved in innate immune response such as ISG15, IL1B, LYN, COPS5, TBK1, MRPL3, and KRAS were found to be critical regulatory hubs in condition B, enzymes involved in amino acid metabolism such as GOT1, PSAT1, AARS, CBS, IMPDH1; subunit of RNA polymerase II (POLR21), plasma membrane-associated Rho GTPase RAC1 and PRKCD were found to critical regulatory proteins in condition C. Interestingly, a previous study exploring the role of kinases in monocyte-macrophage differentiation observed a pronounced decrease in the expression of regulatory kinases such as CDK1 involved in cell cycle entry and checkpoint in PMA-differentiated THP-1 macrophage-like cells (22). It is well known that PMA activates protein kinase C (PKC) and promotes leukocyte adhesion and migration, and therefore identifying PRKCD as one of the regulatory hubs is indicative of the monocyte-to-macrophage differentiation process.

Further investigation on the effect of PMA differentiation protocols on the extent of expression of other protein kinases as well as phosphatases revealed increased expression of several kinases belonging to diverse classes (**Figure 4B**). Notably, protein tyrosine kinases such as CSF1R and PTK2 was overexpressed in condition A, FGR, a member of the c-Src family tyrosine kinases known to be induced by PMA (33-35) in condition B, and BTK2 in condition C, respectively. Interestingly, increased expression of several kinases was observed in condition C including members of the protein kinase C family-PRKCB, PRKCD which are known markers of immune cell differentiation and inflammation, MAP kinase-interacting serine/threonine-protein kinase 1 (MKNK1), MAPK14 and WNK1, a known regulator of ion transport proteins involved in the differentiation and migration of endometrial stromal cells (36) and glioma cells (37). Among the protein phosphatases, 80 were identified and quantified in our dataset, with a vast majority expressed to a similar extent in all conditions tested. Of note,

phosphatases belonging to the HP2 family namely: prostatic acid phosphatase ACPP and acid phosphatase 2 (ACP2), were significantly dysregulated in expression with ACPP over 20-fold overexpressed in condition C with similar level of expression observed in conditions A and B. On the contrary, ACP2, a lysosomal acid phosphatase was overexpressed 2-fold higher in condition A compared to both condition B and C. Among the dual specificity protein phosphatases (DUSPs), SSH3, a member of the slingshot family was upregulated in condition C. SSH3 is known to specifically dephosphorylate and activate Cofilin, one of the key regulators of actin filament dynamics and remodeling (38). Of the 16 protein tyrosine phosphatases (PTPs) identified, the expression of PTPN7, PTPRC were high in condition C whereas PTPN12, PTPN23, PTPN2, PTPRA, PTPRK, and PTPRU were overexpressed in condition A. Interestingly, PTPRE and to a smaller extent, PTPN6 demonstrated increased expression in condition B. Collectively, the protein kinases and phosphatases identified in this study indicate their differential capacity in the regulation of microtubule stability, actin cytoskeleton reorganization and autophagy in macrophages which in turn are required for their functional responses including phagocytosis, antigen presentation, DAMP and PAMP mediated immune signaling.

PMA-induced monocyte-to macrophage differentiation modulates the expression dynamics proteins involved in innate immune signaling

Several previous studies have used THP-1 cells as a model for the immune modulation approach; therefore, we assessed the impact of differentiation protocols on the expression of proteins involved in innate immune signaling. Analysis of the expression profile of proteins involved in Toll-like receptor (TLR) signaling pathways identified several known downstream effector proteins (**Figure 5A, Supplementary Table 8**). A majority were expressed at similar levels in all three conditions, suggesting that the effect of following secondary inflammatory stimuli would be mostly independent of PMA stimulation. Among the TLR receptors, we

identified only TLR2 with over 2-fold expression in conditions A and B. TLR4 co-receptors, namely CD14 and CD180, were found to be expressed relatively lower extent in conditions A and B. CD14 also known as monocyte marker is downregulated upon differentiation. The other signaling regulators and adaptor proteins such as CNPY3 and UN93B1 and CD36 were in general upregulated in condition A in comparison to conditions B and C.

Signaling mediated by TLRs requires the assembly of the Myddosome complex. Although we identified Myd88 (39), quantitation was obtained in only conditions A and B. The other components including IRAK1, IRAK4 and TRAF6 were overexpressed in condition B with slightly increased expression in condition A compared to condition C. Of the transcription factors essential for mediating TLR activity, we observed increased expression in mostly conditions A and B with JUNB, highly expressed in condition B. RelB, a member of NF-κB family, was identified in only conditions A and B (40, 41). The expression of Interferon regulatory transcription factors also varied across the conditions tested with over 4-fold expression IRF3 expression in condition B in comparison to conditions A and C whereas IRF5, a key regulator of antiviral immune response, was 2-fold overexpressed in condition C with respect to conditions A and B.This indicates that using condition C to study TLR signaling and/or non-canonical NF-κB signaling pathway may likely alter the outcome of the experiment, and the subsequent phenotype will mostly be dependent on the PMA stimulation. The expression of kinases belonging to the MAPK family, as described in the earlier section, was generally higher in conditions A and B with the exception of MKNK1, MAP2K1, and MAPK14 which were observed to be upregulated in condition C (**Figure 5A**). Our results are in concordance with a previous report suggesting rewiring of MAPK signaling cascade upon THP1 differentiation (22). We also identified 5 proteins known to be a part of the inflammasome complex that were expressed at similar levels except for NLRP3 that was found to be expressed only in condition B (**Supplementary Figure 6**). We also observed differential

443 expression of proteins known to be involved in the process of phagocytosis and oxidative stress
444 such as FGR, LYN, and pro-inflammatory cytokine IL1B among others which were selectively
445 upregulated in condition B. However, neutrophil cytosolic factors NCF2 and NCF4-regulatory
446 components of the superoxide-producing phagocyte NADPH-oxidase, PYCARD, ITGAL,
447 protein kinase C delta (PRKCD), PTPRC, were found to be upregulated in condition C
448 (**Supplementary Figure 6**). Taken together, our analysis provides insights on the differential
449 expression of immune signaling mediators, transcription factors and effectors that can
450 determine the outcome of the signaling responses following the type of differentiation protocol
451 employed.
452 The response of activated macrophages by various stimuli involves the secretion of cytokines
453 such as IL-1β, IL-6, IL-8, and TNF-α as a significant component of the innate immune response
454 (42). We, therefore, studied the functional properties, cytokine gene expression in
455 undifferentiated (monocytic), and differentially differentiated THP1 cells (macrophage-like)
456 and compared the dissimilarity and similarity of expression trends among conditions. To assess
457 the changes in the cytokine mRNA expression levels, cells were treated with various TLR
458 ligands: CL075-TLR7/8, CpG2006-TLR9, Flagellin-TLR5, FSL1-TLR2/6, LPS 0111:B4, and
459 LPS K12 – TLR4, Pam3CSK4-TLR2/1, Poly I:C-TLR3, R837-TLR7, and R848-TLR7/8
460 (**Figure 5B**). Monocytes are the first cells that encounter pathogens and promptly adapt to the
461 environmental situations by regulating the expression of genes activated by the inflammasome,
462 such as IL-1β (43). As anticipated, the TLR2 ligand Pam3CSK4 stimulated undifferentiated
463 cells showed significant cytokine induction of *IL1β* mRNA. Interestingly, it also induced a high
464 level of *IL6* and *IL8*. On the other hand, the average cytokine expression appeared to increase
465 in PMA differentiated cells with respect to the undifferentiated cells, except when it was
466 simulated with CpG2006, Flagellin, and R848. Expression of cytokines upon stimulation with
467 FSL1, LPS 0111: B4, LPS K12, and Pam3CSK4 did not significantly vary among the different

differentiation conditions except for *IL6* mRNA which was markedly downregulated upon CpG2006, Flagellin and R848 stimulation in condition A. Overall, the most robust upregulation, especially with respect to *IL6* and *TNF-α* expression levels were observed in condition B (**Figure 5B**). Together these experiments indicate that depending on the context of the experimental question, careful consideration of the differentiation protocols selection must be made to avoid undesired outcomes.

Discussion

Human monocytic THP-1 cells are extensively used as a model system to study monocyte/macrophage functions. However, to be used as an *in vitro* model mimicking human macrophages, THP-1 cells have to be differentiated, and several protocols have been tested (7, 9, 29, 44). Among these, PMA is most often employed to induce differentiation, with almost similar phenotypes reported in terms of cell morphology, expression of macrophage surface markers, and cytokine production (28, 45). However, the amount and duration of incubation with PMA vary widely across the literature. Additionally, studies demonstrate altered sensitivity, as well as undesirable gene regulation in PMA-differentiated macrophages that may contribute to their differential response to secondary stimuli (12, 28). Although this may likely be the case, one inherent limitation of most of these studies is that their focus has primarily been on characterizing either the transcriptional profile or surface receptor expression (11, 30). Since the effect of any stimuli is a global response, it is imperative to study the impact of differentiation at the global proteome level.

To illustrate changes in the proteome expression dynamics during differentiation of THP-1 cells into macrophage-like cells, we performed a global quantitative proteomic analysis by comparing three established and widely employed PMA-mediated differentiation protocols. Our analysis indicates that in the course of monocyte to macrophage differentiation, the proteome profiles across the three tested protocols display common and differentiation-protocol-specific regulation with the expression of known macrophage differentiation markers significantly induced in two of the three conditions. We also delineated the biological and cellular processes that are impacted to a considerable extent depending on the type of treatment conditions. Importantly, regulation of immune signaling response, protein transport, and regulation of cell migration, all indicative of macrophage function were significantly enriched in conditions A and B. These treatment conditions include the use of a higher concentration of

PMA, followed by a period of rest appeared to correlate well with macrophage-like phenotype, unlike what was suggested previously (12).

GM-CSF-mediated differentiation of primary human monocytes to macrophages upregulates the macrophage-specific surface markers/receptors, antigen-presenting function, phagocytosis, anti-microbial activity, lipid metabolism and production of growth factors and pro-inflammatory cytokines as evidenced by the global transcriptome analysis of GM-CSF-induced macrophages (46). We too observed a similar trend with treatment condition B showing a better representation of proteins involved in innate immune signaling while cathepsins- proteases involved in innate immune responses and protein kinases involved in the processes of cell proliferation and differentiation (47, 48) were found to be significantly induced in condition A. The increased expression of *IL1B* upon PMA differentiation has been reported earlier at the transcriptome level (11). Although we did not examine the phagocytic activity of differentiated macrophages in this study, we provide evidence of differential expression of proteins involved in the process of phagocytosis across the three tested protocols. Importantly, proteins including kinases, members of Rho GTPase family and adaptors involved in the formation of lamellopodia and actin cytoskeleton reorganization among others were found to be upregulated in conditions A and B (49). On the contrary, regulatory components of the superoxide-producing phagocyte NADPH-oxidase were upregulated in condition C. Our analysis also resulted in the identification of several integrins, known to be involved in the processes of cell adhesion and cell surface receptor-mediated signaling required to maintain homeostasis as well as host defense and inflammation (50). Although the extent of expression of integrins were almost similar, differential induction of CD49c (ITGA3) and ITGB1 (CD29) (50), were observed in condition A with respect to others. ITGAL (CD11a), a pan-leukocyte marker was found to be upregulated in condition C compared to the other two tested protocols indicating

that the differential expression may likely contribute to differences in the initiation of primary immune response (50).

Our analysis further highlights differentiation protocol-specific subsets with several protein kinases serving as central hubs in mediating the differentiation process. This is of vital importance as cellular signaling is largely governed by the regulation of expression of kinases and phosphatases in a cell type-specific manner or upon cell activation (51-53). One of the major findings of this study is the differential expression of key regulatory kinases implicated in cell cycle regulation including cyclin-dependent kinases, NEK family of serine-threonine kinases as well as cAMP/PKA-induced signaling that are collectively responsible for enrichment of signaling pathways involved in differentiation, maturation, and regulation of actin cytoskeleton dynamics (54, 55). Interestingly, a pronounced decrease in the expression of vital regulatory kinases in cell cycle entry and checkpoint including the cyclin-dependent kinases has been reported in a previous study exploring the role of kinases in monocyte-macrophage differentiation (22). Similarly, the members of protein kinase C family of serine- and threonine kinases are known to phosphorylate a wide range of proteins involved in cell maintenance and also serve as receptors for phorbol esters (56). We observed several members of this family to be significantly overexpressed in condition C with respect to the other conditions. The observed effect may be attributed to these cells being in a transition state and therefore, do not demarcate as monocyte/macrophage populations. Results from previous studies also indicate that the monocyte to macrophage differentiation is accompanied by extensive rewiring of the MAPK-signaling cascades (22). This was partly observed in our analysis as well with MAPK1 identified as a key regulatory hub in condition A. As reported earlier, we too observed a moderate increase in the expression of MAP2K3, MAP3K2 and MAP3K7 in conditions A and B in comparison to condition C, thereby confirming that these two protocols induced the differentiation to macrophage-like cells (22).

548 Cytokine responses induced in monocytes and macrophages are known to vary depending on
549 the stimulus and the type of differentiated macrophage studied. Overall, we observed an
550 increase transcriptional response of pro-inflammatory cytokines upon stimulation with TLR
551 ligands except for R848- a TLR8 agonist and CPG2006, a TLR9 agonist, which showed an
552 overall decrease in the expression of cytokine mRNA expression especially *IL6* mRNA in
553 condition A and C respectively. Between the three different protocols, no apparent differences
554 in the induction of cytokines were observed in the case of flagellin (TLR5 agonist), poly I:C
555 (TLR3 agonist), and LPS (TLR4 agonist). The consensus on the induction of *TNF*α by LPS in
556 monocytes and macrophages remains unclear as some studies report higher induction in
557 monocytes, whereas others report the same in macrophages, and these differences may likely
558 be attributed to the differentiation protocols and purity and type of the ligands. Using rough
559 and smooth LPS, we demonstrate an increased induction of all pro-inflammatory cytokines in
560 all the three protocols tested with sustained increased expression observed in condition B. We
561 also noted that the more differentiated macrophage-like cells had higher *TNFα* inducible
562 responses to the TLR2 agonist Pam3CSK4. On the contrary, the induction of *IL1β* by
563 Pam3CSK4 was downregulated with respect to undifferentiated monocytes in all the three
564 protocols tested. Taken together, our findings suggest that TLR ligands induce comparable
565 levels of cytokine gene expression across the protocols tested with condition B.
566 In conclusion, conditions A and B were found to express the most number of macrophage
567 markers, and desirable characteristics such as increased expression of cell surface receptors
568 and differentiation markers, increased expression of proteins involved in innate immune
569 signaling, and overall similar responses to TLR ligands. This suggests that the extended
570 duration of rest post PMA treatment may not directly contribute to significant alterations in the
571 proteome expression. Although both expressed a distinct set of proteins, a vast majority of
572 cellular processes, including metabolic responses, were mostly unaffected, suggesting that

573 metabolic reprogramming effects observed during secondary stimuli would be independent of
574 the PMA response. This suggests that of the tested conditions, condition B is the most optimal
575 differentiation protocol to studying innate immune signaling. Minor deviations in the protocols
576 can have unintended effects on the overall experimental setup and subsequently on the results.
577 Therefore, validation of the model solely by means of morphological or cell surface expression
578 of select markers may not suffice and should be supplemented with orthogonal experiments
579 that provide a more significant overview of the cellular state. The present datasets, in particular,
580 the quantitative differences in the proteome repertoire of molecules involved in innate immune
581 signaling, represent a valuable resource to understand and modulate the functionality of
582 monocyte-derived macrophages.

Acknowledgments

LC-MS data acquisition was performed at the Proteomics and Modomics Experimental Core Facility (PROMEC), Norwegian University of Science and Technology (NTNU). PROMEC is funded by the Faculty of Medicine and Health Sciences at NTNU and the Central Norway Regional Health Authority. Data storage and handling are supported under the NIRD/Notur project NN9036K. We thank Lars Hagen, Animesh Sharma, and Aditya Kumar Sharma for their technical assistance and Geir Slupphaug for his continued support.

Funding

This research was funded by the Research Council of Norway (FRIMEDBIO "Young Research Talent" Grant 263168 to R.K.K.; and Centres of Excellence Funding Scheme Project 223255/F50 to CEMIR), Onsager fellowship from NTNU (to R.K.K.), and Regional Health Authority of Central Norway (90414000 to KB).

Abbreviations

BCA	Bicinchoninic Acid
DTT	Dithiothreitol
FACS	Fluorescence-Activated Cell Sorting
GO	Gene Ontology
HCD	Higher-energy Collisional Dissociation
IAA	Iodoacetamide
MS/MS	Tandem mass spectrometry
PCA	Principal Component Analysis
PMA	Phorbol-12-myristate-13- acetate
SCX	Strong Cation Exchange
TLR	Toll-Like Receptor
UHPLC	Ultra-High-Performance Liquid Chromatography

609 **Figure legends**

610 **Figure 1: Changes in cell morphology and surface receptor expression are dependent on**
611 **PMA- mediated differentiation conditions**

612 (A). Representative bright-field images (Scale bar:100 μm) (B) Representative forward and
613 side light scatter plot (C) Representative flow cytometric analysis of THP-1 cells stained using
614 anti- CD86, CD11b or -CD14 of THP-1 cells differentiated with varying concentration of PMA
615 (Condition A: 50ng/ml PMA 72h, +48h rest, Condition B: 50ng/ml PMA overnight, + 48h rest
616 and Condition C: 5 ng/ml PMA 48h, +3h rest). Data is representative of at least three
617 independent experiments

618 **Figure 2: Quantitative proteomic analysis of PMA-induced changes**

619 (A) The experimental strategy employed for comparative proteome analysis in response to
620 varying PMA-mediated differentiation protocols. Dimethyl labeling-based quantitative
621 proteomic approach was employed to identify and quantify the proteome changes in Condition
622 A (Light), Condition B (Medium), and Condition C (Heavy).The data were acquired in
623 biological quadruplicates and only proteins identified and quantified in all 4 replicates were
624 considered for further analysis.

625 (B) Principal component analysis (PCA) reveals that the three treatment conditions for
626 monocyte-to macrophage differentiation of THP-1 cells segregate from each on the basis of
627 concentration and duration of PMA treatment. All replicates of a given condition cluster
628 together suggesting minimal biological variability.

629 (C-E) Volcano plot displaying differential expressed proteins between (A) Condition A vs. B
630 (B) Condition C vs. A and (C) Condition C vs. B. The vertical axis (y-axis) corresponds to the
631 mean expression value of log 10 (q-value), and the horizontal axis (x-axis) displays the log 2-
632 fold change value. The red dots represent overexpressed proteins, and the green dots represent

proteins with downregulated expression. Positive x-values represent overexpression, and negative x-values represent down-regulation.

Figure 3: Protein expression dynamics analysis upon PMA induced monocyte to macrophage differentiation

(A) Protein expression patterns in response to differentiation protocols A, B, and C were analyzed. Log2 transformed, z-score normalized and scaled expression of proteins identified and quantified in all replicated were plotted, and k-means clustering was carried out. K-means clusters 1, 7 and 9 which showed overexpressed proteins exclusive to conditions A, B, and C, have been highlighted.

(B) The proteins exclusive to each condition were subjected to Gene Ontology (GO) analysis using Enrichr to understand their function. Selected significantly enriched GO terms (biological processes) ($p\text{-value} \leqslant 0.005$) have been highlighted.

Figure 4: Gene ontology analysis of proteins upon PMA induced monocyte to macrophage differentiation

(A) Gene Ontology analysis of upregulated and downregulated proteins in conditions A, B, and C using ReactomePA.

(B). Kinome trees showing differential regulation of protein kinases in response to differentiation conditions A, B, and C. The phylogenetic kinase relationship (Manning et al., 2002) were generated using KinMap. Protein kinases identified and quantified in our study are indicated as gray and black circles, respectively.

Figure 5: Expression dynamics of genes involved in innate immune signaling in response to PMA

(A) Heatmap showing the proteome fold change of the subset of genes involved in innate immune signaling. Scale indicates the level of expression (Log2-expression values, z-transformed, scaled).

658 (B) Dynamic expression pattern to assess the expression levels of pro-inflammatory cytokine
659 mRNA induced by TLR agonists: CL075-TLR7/8, CpG2006-TLR9, Flagellin-TLR5, FSL1-
660 TLR2/6, LPS 0111:B4, and LPS K12 – TLR4, Pam3CSK4-TLR2/1, Poly I:C-TLR3, R837-
661 TLR7, and R848-TLR7/8. Heatmap depicts Log10 fold change of normalized gene expression
662 for pairwise comparisons of mRNA levels.
663

664 **References:**

665 1. Taylor, P. R., and S. Gordon. 2003. Monocyte heterogeneity and innate immunity.
666 *Immunity* 19: 2-4.
667 2. Gordon, S. 1998. The role of the macrophage in immune regulation. *Res Immunol* 149:
668 685-688.
669 3. Gordon, S. 1986. Biology of the macrophage. *J Cell Sci Suppl* 4: 267-286.
670 4. Gordon, S., and P. R. Taylor. 2005. Monocyte and macrophage heterogeneity. *Nat Rev*
671 *Immunol* 5: 953-964.
672 5. Auwerx, J. 1991. The human leukemia cell line, THP-1: a multifacetted model for the
673 study of monocyte-macrophage differentiation. *Experientia* 47: 22-31.
674 6. Chanput, W., J. J. Mes, and H. J. Wichers. 2014. THP-1 cell line: an in vitro cell model
675 for immune modulation approach. *Int Immunopharmacol* 23: 37-45.
676 7. Daigneault, M., J. A. Preston, H. M. Marriott, M. K. Whyte, and D. H. Dockrell. 2010.
677 The identification of markers of macrophage differentiation in PMA-stimulated THP-
678 1 cells and monocyte-derived macrophages. *PLoS One* 5: e8668.
679 8. Qin, Z. 2012. The use of THP-1 cells as a model for mimicking the function and
680 regulation of monocytes and macrophages in the vasculature. *Atherosclerosis* 221: 2-
681 11.
682 9. Tsuchiya, S., Y. Kobayashi, Y. Goto, H. Okumura, S. Nakae, T. Konno, and K. Tada.
683 1982. Induction of maturation in cultured human monocytic leukemia cells by a phorbol
684 diester. *Cancer Res* 42: 1530-1536.
685 10. Cavaillon, J. M. 1994. Cytokines and macrophages. *Biomed Pharmacother* 48: 445-
686 453.
687 11. Kohro, T., T. Tanaka, T. Murakami, Y. Wada, H. Aburatani, T. Hamakubo, and T.
688 Kodama. 2004. A comparison of differences in the gene expression profiles of phorbol

12-myristate 13-acetate differentiated THP-1 cells and human monocyte-derived macrophage. *J Atheroscler Thromb* 11: 88-97.

12. Park, E. K., H. S. Jung, H. I. Yang, M. C. Yoo, C. Kim, and K. S. Kim. 2007. Optimized THP-1 differentiation is required for the detection of responses to weak stimuli. *Inflamm Res* 56: 45-50.

13. Valle, E., and D. G. Guiney. 2005. Characterization of Salmonella-induced cell death in human macrophage-like THP-1 cells. *Infect Immun* 73: 2835-2840.

14. Aldo, P. B., V. Craveiro, S. Guller, and G. Mor. 2013. Effect of culture conditions on the phenotype of THP-1 monocyte cell line. *Am J Reprod Immunol* 70: 80-86.

15. Tedesco, S., F. De Majo, J. Kim, A. Trenti, L. Trevisi, G. P. Fadini, C. Bolego, P. W. Zandstra, A. Cignarella, and L. Vitiello. 2018. Convenience versus Biological Significance: Are PMA-Differentiated THP-1 Cells a Reliable Substitute for Blood-Derived Macrophages When Studying in Vitro Polarization? *Front Pharmacol* 9: 71.

16. Weber, C., K. U. Belge, P. von Hundelshausen, G. Draude, B. Steppich, M. Mack, M. Frankenberger, K. S. Weber, and H. W. Ziegler-Heitbrock. 2000. Differential chemokine receptor expression and function in human monocyte subpopulations. *J Leukoc Biol* 67: 699-704.

17. Passlick, B., D. Flieger, and H. W. Ziegler-Heitbrock. 1989. Identification and characterization of a novel monocyte subpopulation in human peripheral blood. *Blood* 74: 2527-2534.

18. Ziegler-Heitbrock, H. W., G. Fingerle, M. Strobel, W. Schraut, F. Stelter, C. Schutt, B. Passlick, and A. Pforte. 1993. The novel subset of CD14+/CD16+ blood monocytes exhibits features of tissue macrophages. *Eur J Immunol* 23: 2053-2058.

19. Zeng, C., W. Wang, X. Yu, L. Yang, S. Chen, and Y. Li. 2015. Pathways related to PMA-differentiated THP1 human monocytic leukemia cells revealed by RNA-Seq. *Sci China Life Sci* 58: 1282-1287.

20. Abe, T., M. Ohno, T. Sato, M. Murakami, M. Kajiki, and R. Kodaira. 1991. "Differentiation Induction" culture of human leukemic myeloid cells stimulates high production of macrophage differentiation inducing factor. *Cytotechnology* 5: 75-93.

21. Court, M., G. Petre, M. E. Atifi, and A. Millet. 2017. Proteomic Signature Reveals Modulation of Human Macrophage Polarization and Functions Under Differing Environmental Oxygen Conditions. *Mol Cell Proteomics* 16: 2153-2168.

22. Richter, E., K. Ventz, M. Harms, J. Mostertz, and F. Hochgrafe. 2016. Induction of Macrophage Function in Human THP-1 Cells Is Associated with Rewiring of MAPK Signaling and Activation of MAP3K7 (TAK1) Protein Kinase. *Front Cell Dev Biol* 4: 21.

23. Kalxdorf, M., S. Gade, H. C. Eberl, and M. Bantscheff. 2017. Monitoring Cell-surface N-Glycoproteome Dynamics by Quantitative Proteomics Reveals Mechanistic Insights into Macrophage Differentiation. *Mol Cell Proteomics* 16: 770-785.

24. Kulak, N. A., G. Pichler, I. Paron, N. Nagaraj, and M. Mann. 2014. Minimal, encapsulated proteomic-sample processing applied to copy-number estimation in eukaryotic cells. *Nat Methods* 11: 319-324.

25. Livak, K. J., and T. D. Schmittgen. 2001. Analysis of relative gene expression data using real-time quantitative PCR and the 2(-Delta Delta C(T)) Method. *Methods* 25: 402-408.

26. Vizcaino, J. A., A. Csordas, N. del-Toro, J. A. Dianes, J. Griss, I. Lavidas, G. Mayer, Y. Perez-Riverol, F. Reisinger, T. Ternent, Q. W. Xu, R. Wang, and H. Hermjakob.

2016. 2016 update of the PRIDE database and its related tools. *Nucleic Acids Res* 44: D447-456.

27. Yurchenko, M., A. Skjesol, L. Ryan, G. M. Richard, R. K. Kandasamy, N. Wang, C. Terhorst, H. Husebye, and T. Espevik. 2018. SLAMF1 is required for TLR4-mediated TRAM-TRIF-dependent signaling in human macrophages. *J Cell Biol* 217: 1411-1429.

28. Starr, T., T. J. Bauler, P. Malik-Kale, and O. Steele-Mortimer. 2018. The phorbol 12-myristate-13-acetate differentiation protocol is critical to the interaction of THP-1 macrophages with Salmonella Typhimurium. *PLoS One* 13: e0193601.

29. Schwende, H., E. Fitzke, P. Ambs, and P. Dieter. 1996. Differences in the state of differentiation of THP-1 cells induced by phorbol ester and 1,25-dihydroxyvitamin D3. *J Leukoc Biol* 59: 555-561.

30. Forrester, M. A., H. J. Wassall, L. S. Hall, H. Cao, H. M. Wilson, R. N. Barker, and M. A. Vickers. 2018. Similarities and differences in surface receptor expression by THP-1 monocytes and differentiated macrophages polarized using seven different conditioning regimens. *Cell Immunol* 332: 58-76.

31. Maniecki, M. B., A. Etzerodt, S. K. Moestrup, H. J. Moller, and J. H. Graversen. 2011. Comparative assessment of the recognition of domain-specific CD163 monoclonal antibodies in human monocytes explains wide discrepancy in reported levels of cellular surface CD163 expression. *Immunobiology* 216: 882-890.

32. Buechler, C., M. Ritter, E. Orso, T. Langmann, J. Klucken, and G. Schmitz. 2000. Regulation of scavenger receptor CD163 expression in human monocytes and macrophages by pro- and antiinflammatory stimuli. *J Leukoc Biol* 67: 97-103.

33. Faulkner, L., M. Patel, P. M. Brickell, and D. R. Katz. 1997. The role of the Fgr tyrosine kinase in the control of the adhesive properties of U937 monoblastoid cells and their derivatives. *Immunology* 92: 519-526.

761 34. Faulkner, L., M. Patel, P. M. Brickell, and D. R. Katz. 1992. Regulation of c-fgr
762 messenger RNA levels in U937 cells treated with different modulating agents.
763 *Immunology* 76: 65-71.
764 35. Kefalas, P., T. R. Brown, D. R. Katz, and P. M. Brickell. 1995. Identification of a
765 phorbol ester responsive region in the myeloid-specific promoter of the c-fgr proto-
766 oncogene. *Biochem Biophys Res Commun* 209: 60-65.
767 36. Adams, N. R., Y. M. Vasquez, Q. Mo, W. Gibbons, E. Kovanci, and F. J. DeMayo.
768 2017. WNK lysine deficient protein kinase 1 regulates human endometrial stromal cell
769 decidualization, proliferation, and migration in part through mitogen-activated protein
770 kinase 7. *Biol Reprod* 97: 400-412.
771 37. Zhu, W., G. Begum, K. Pointer, P. A. Clark, S. S. Yang, S. H. Lin, K. T. Kahle, J. S.
772 Kuo, and D. Sun. 2014. WNK1-OSR1 kinase-mediated phospho-activation of Na+-K+-
773 2Cl- cotransporter facilitates glioma migration. *Mol Cancer* 13: 31.
774 38. Niwa, R., K. Nagata-Ohashi, M. Takeichi, K. Mizuno, and T. Uemura. 2002. Control
775 of actin reorganization by Slingshot, a family of phosphatases that dephosphorylate
776 ADF/cofilin. *Cell* 108: 233-246.
777 39. Deguine, J., and G. M. Barton. 2014. MyD88: a central player in innate immune
778 signaling. *F1000Prime Rep* 6: 97.
779 40. Sun, S. C. 2011. Non-canonical NF-kappaB signaling pathway. *Cell Res* 21: 71-85.
780 41. Kawai, T., and S. Akira. 2007. Signaling to NF-kappaB by Toll-like receptors. *Trends*
781 *Mol Med* 13: 460-469.
782 42. Arango Duque, G., and A. Descoteaux. 2014. Macrophage cytokines: involvement in
783 immunity and infectious diseases. *Front Immunol* 5: 491.

784 43. Netea, M. G., A. Simon, F. van de Veerdonk, B. J. Kullberg, J. W. Van der Meer, and
785 L. A. Joosten. 2010. IL-1beta processing in host defense: beyond the inflammasomes.
786 *PLoS Pathog* 6: e1000661.
787 44. Chen, Q., and A. C. Ross. 2004. Retinoic acid regulates cell cycle progression and cell
788 differentiation in human monocytic THP-1 cells. *Exp Cell Res* 297: 68-81.
789 45. Lund, M. E., J. To, B. A. O'Brien, and S. Donnelly. 2016. The choice of phorbol 12-
790 myristate 13-acetate differentiation protocol influences the response of THP-1
791 macrophages to a pro-inflammatory stimulus. *J Immunol Methods* 430: 64-70.
792 46. Lehtonen, A., H. Ahlfors, V. Veckman, M. Miettinen, R. Lahesmaa, and I. Julkunen.
793 2007. Gene expression profiling during differentiation of human monocytes to
794 macrophages or dendritic cells. *J Leukoc Biol* 82: 710-720.
795 47. Liu, Y., H. Liu, H. Cao, B. Song, W. Zhang, and W. Zhang. 2015. PBK/TOPK mediates
796 promyelocyte proliferation via Nrf2-regulated cell cycle progression and apoptosis.
797 *Oncol Rep* 34: 3288-3296.
798 48. Abshire, M. Y., K. S. Thomas, K. A. Owen, and A. H. Bouton. 2011. Macrophage
799 motility requires distinct alpha5beta1/FAK and alpha4beta1/paxillin signaling events.
800 *J Leukoc Biol* 89: 251-257.
801 49. Afzal, T. A., L. A. Luong, D. Chen, C. Zhang, F. Yang, Q. Chen, W. An, E. Wilkes, K.
802 Yashiro, P. R. Cutillas, L. Zhang, and Q. Xiao. 2016. NCK Associated Protein 1
803 Modulated by miRNA-214 Determines Vascular Smooth Muscle Cell Migration,
804 Proliferation, and Neointima Hyperplasia. *J Am Heart Assoc* 5.
805 50. Ammon, C., S. P. Meyer, L. Schwarzfischer, S. W. Krause, R. Andreesen, and M.
806 Kreutz. 2000. Comparative analysis of integrin expression on monocyte-derived
807 macrophages and monocyte-derived dendritic cells. *Immunology* 100: 364-369.

808 51. Lang, R., and F. A. M. Raffi. 2019. Dual-Specificity Phosphatases in Immunity and
809 Infection: An Update. *Int J Mol Sci* 20.
810 52. Rieckmann, J. C., R. Geiger, D. Hornburg, T. Wolf, K. Kveler, D. Jarrossay, F. Sallusto,
811 S. S. Shen-Orr, A. Lanzavecchia, M. Mann, and F. Meissner. 2017. Social network
812 architecture of human immune cells unveiled by quantitative proteomics. *Nat Immunol*
813 18: 583-593.
814 53. Subbannayya, Y., S. M. Pinto, K. Bosl, T. S. K. Prasad, and R. K. Kandasamy. 2019.
815 Dynamics of Dual Specificity Phosphatases and Their Interplay with Protein Kinases
816 in Immune Signaling. *Int J Mol Sci* 20.
817 54. Chiba, S., Y. Amagai, Y. Homma, M. Fukuda, and K. Mizuno. 2013. NDR2-mediated
818 Rabin8 phosphorylation is crucial for ciliogenesis by switching binding specificity from
819 phosphatidylserine to Sec15. *EMBO J* 32: 874-885.
820 55. Yang, L., F. Dai, L. Tang, Y. Le, and W. Yao. 2017. Macrophage differentiation
821 induced by PMA is mediated by activation of RhoA/ROCK signaling. *J Toxicol Sci* 42:
822 763-771.
823 56. Castagna, M., Y. Takai, K. Kaibuchi, K. Sano, U. Kikkawa, and Y. Nishizuka. 1982.
824 Direct activation of calcium-activated, phospholipid-dependent protein kinase by
825 tumor-promoting phorbol esters. *J Biol Chem* 257: 7847-7851.
826

Figure 1

A

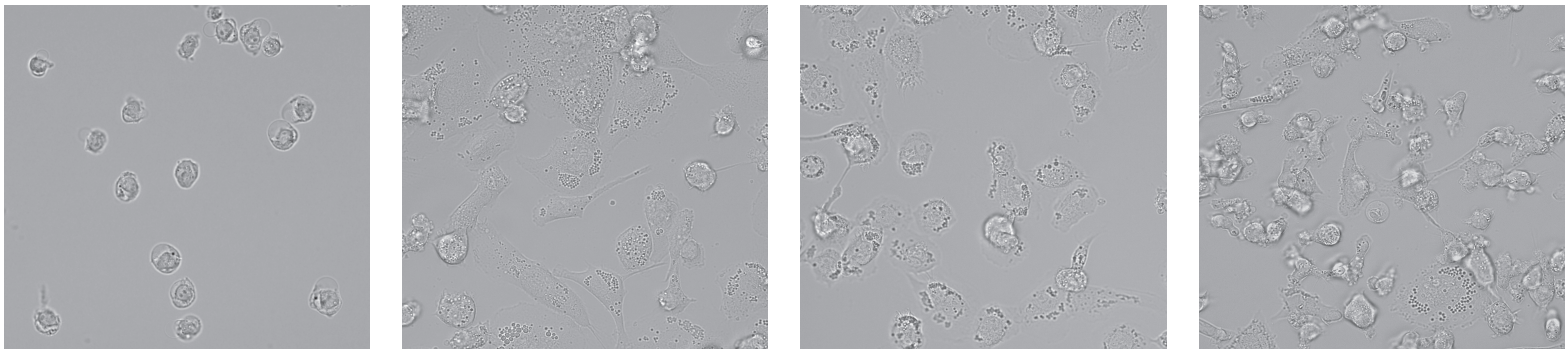
Undifferentiated
Condition A
Condition B
Condition C

B

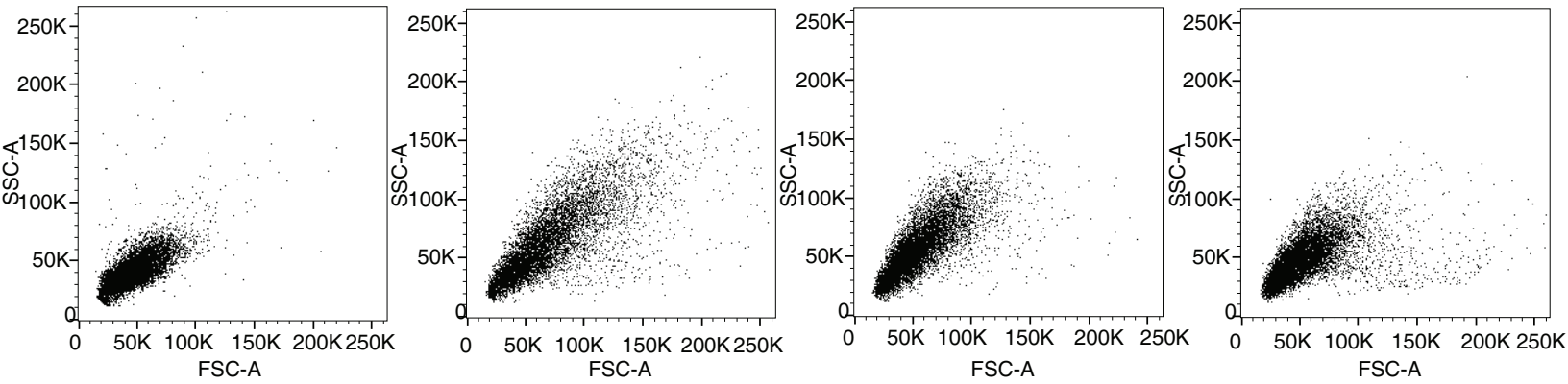
SSC-A
FSC-A
0
50K
100K
150K
200K
250K

C

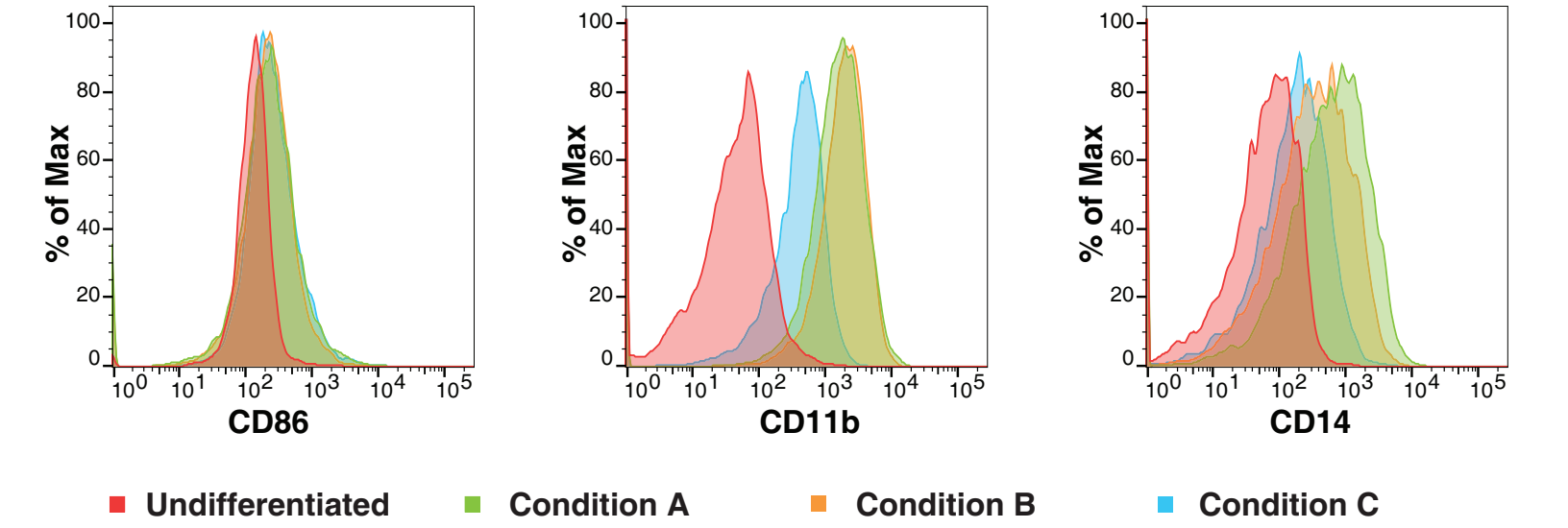
% of Max
CD86
CD11b
CD14
Undifferentiated
Condition A
Condition B
Condition C

Figure 2

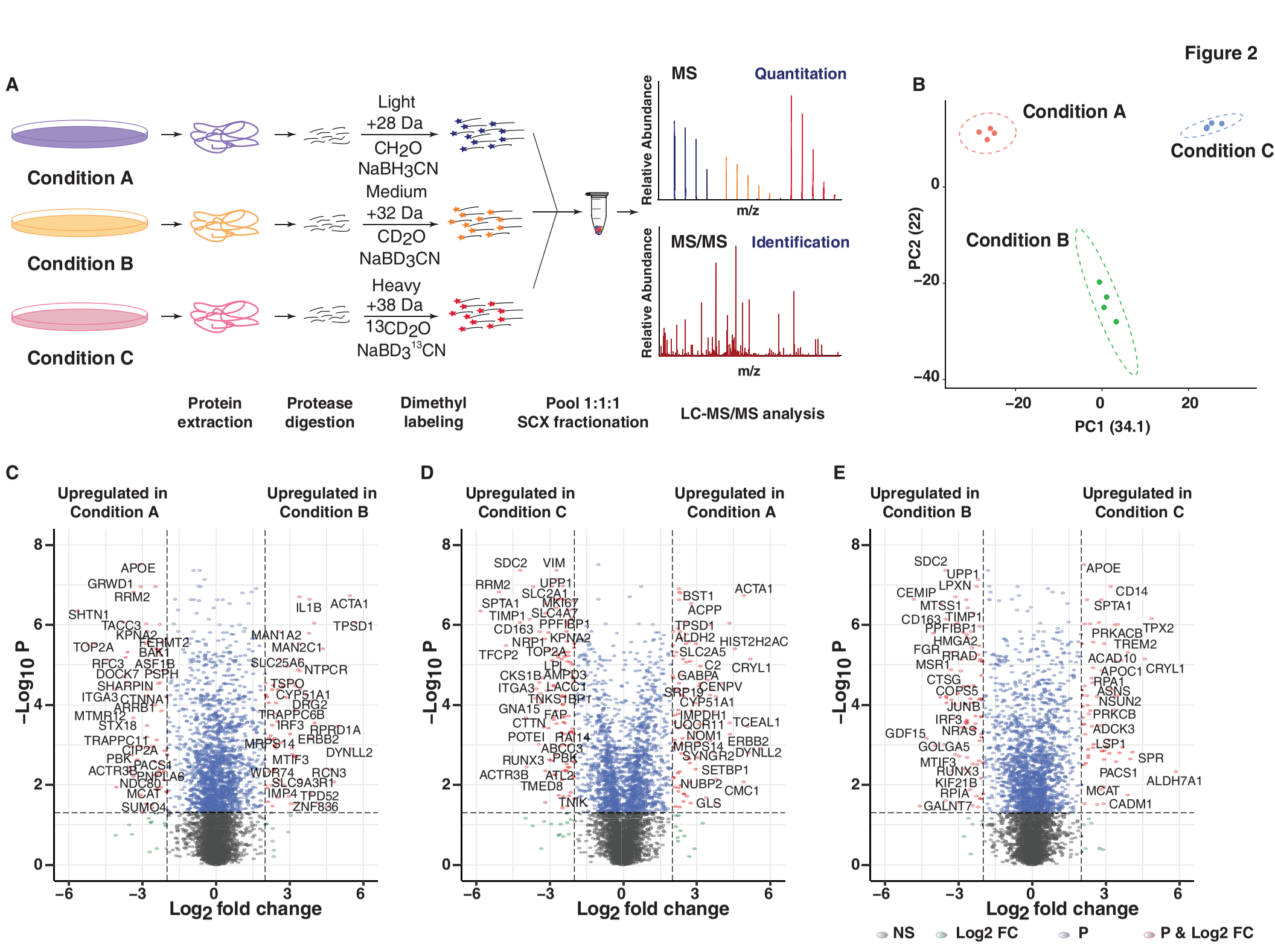
A
Condition A
Condition B
Condition C
Light
+28 Da
CH2O
NaBH3CN
Medium
+32 Da
CD2O
NaBD3CN
Heavy
+38 Da
13CD2O
NaBD3 13CN
MS
Quantitation
Relative Abundance
m/z
MS/MS
Identification
Relative Abundance
m/z
Protein extraction
Protease digestion
Dimethyl labeling
Pool 1:1:1 SCX fractionation
LC-MS/MS analysis
B
Condition A
Condition C
Condition B
PC2 (22)
PC1 (34.1)
C
Upregulated in Condition A
Upregulated in Condition B
−Log10 P
Log2 fold change
D
Upregulated in Condition C
Upregulated in Condition A
−Log10 P
Log2 fold change
E
Upregulated in Condition B
Upregulated in Condition C
−Log10 P
Log2 fold change
NS
Log2 FC
P
P & Log2 FC

Figure 3

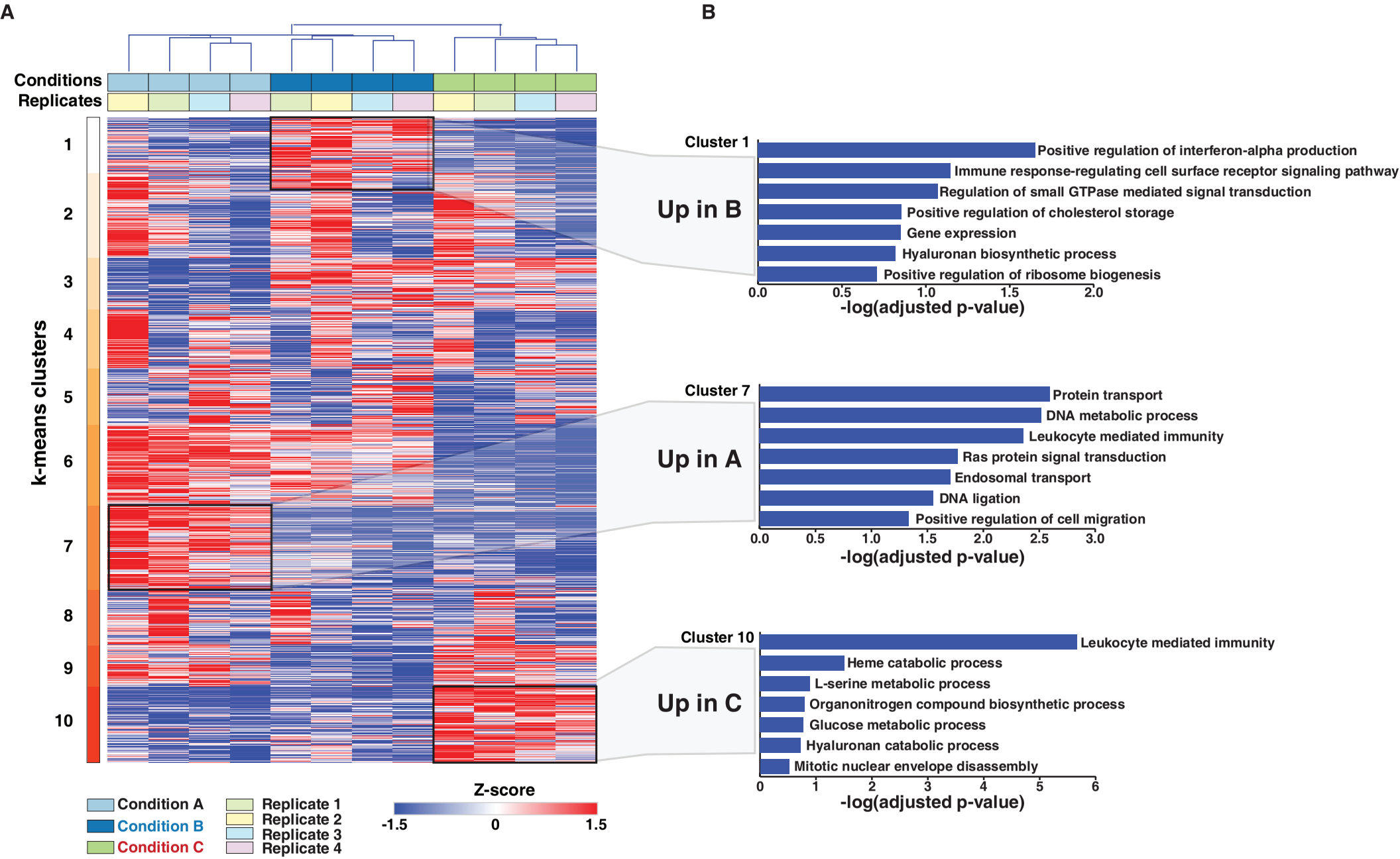
A
Conditions
Replicates
k-means clusters
1
2
3
4
5
6
7
8
9
10
Condition A
Condition B
Condition C
Replicate 1
Replicate 2
Replicate 3
Replicate 4
Z-score
-1.5
0
1.5
B
Cluster 1
Up in B
Positive regulation of interferon-alpha production
Immune response-regulating cell surface receptor signaling pathway
Regulation of small GTPase mediated signal transduction
Positive regulation of cholesterol storage
Gene expression
Hyaluronan biosynthetic process
Positive regulation of ribosome biogenesis
0.0
0.5
1.0
1.5
2.0
-log(adjusted p-value)
Cluster 7
Up in A
Protein transport
DNA metabolic process
Leukocyte mediated immunity
Ras protein signal transduction
Endosomal transport
DNA ligation
Positive regulation of cell migration
0.0
0.5
1.0
1.5
2.0
2.5
3.0
-log(adjusted p-value)
Cluster 10
Up in C
Leukocyte mediated immunity
Heme catabolic process
L-serine metabolic process
Organonitrogen compound biosynthetic process
Glucose metabolic process
Hyaluronan catabolic process
Mitotic nuclear envelope disassembly
0
1
2
3
4
5
6
-log(adjusted p-value)

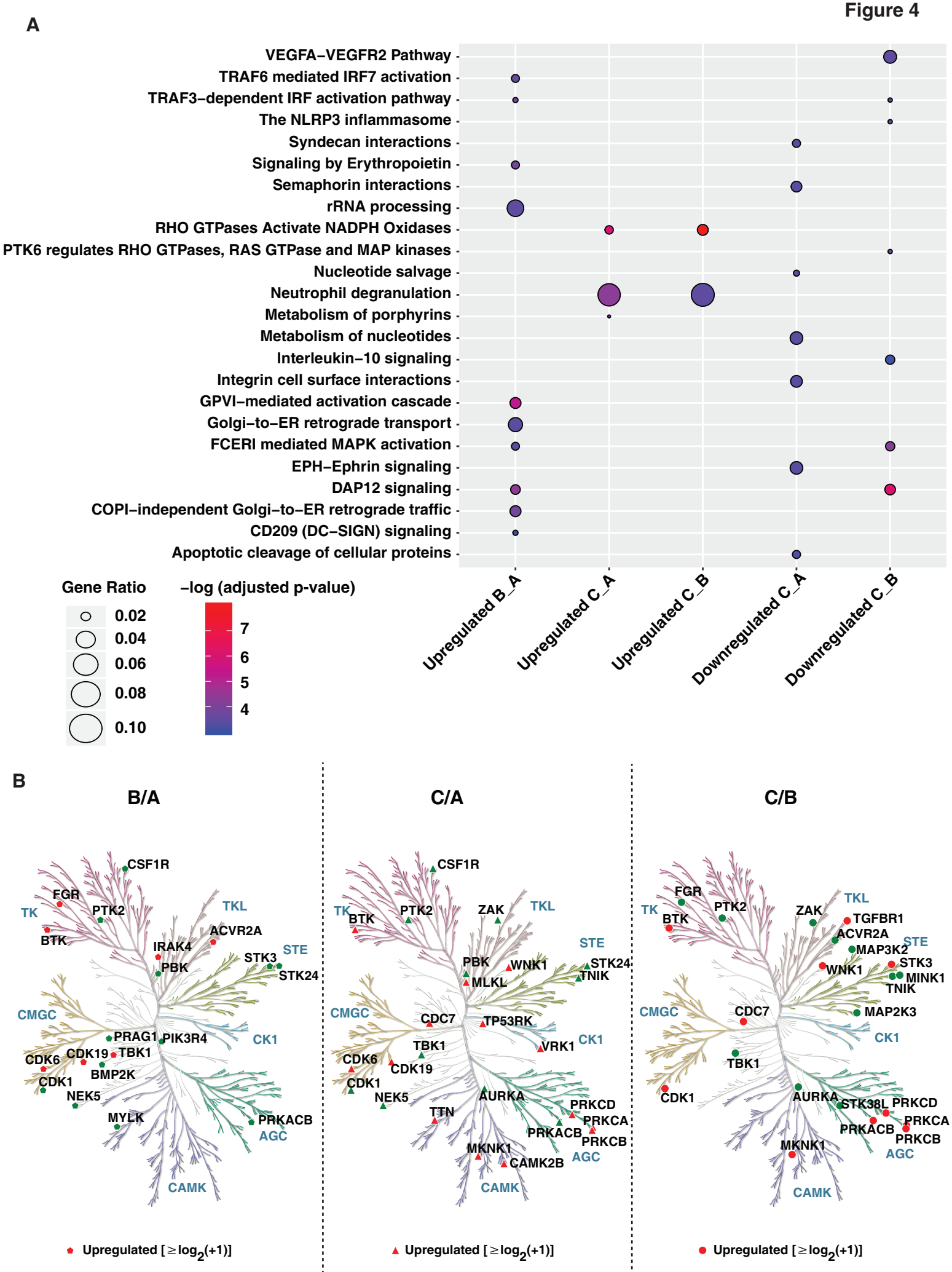
A
VEGFA–VEGFR2 Pathway
TRAF6 mediated IRF7 activation
TRAF3–dependent IRF activation pathway
The NLRP3 inflammasome
Syndecan interactions
Signaling by Erythropoietin
Semaphorin interactions
rRNA processing
RHO GTPases Activate NADPH Oxidases
PTK6 regulates RHO GTPases, RAS GTPase and MAP kinases
Nucleotide salvage
Neutrophil degranulation
Metabolism of porphyrins
Metabolism of nucleotides
Interleukin–10 signaling
Integrin cell surface interactions
GPVI–mediated activation cascade
Golgi–to–ER retrograde transport
FCERI mediated MAPK activation
EPH–Ephrin signaling
DAP12 signaling
COPI–independent Golgi–to–ER retrograde traffic
CD209 (DC–SIGN) signaling
Apoptotic cleavage of cellular proteins
Upregulated B_A
Upregulated C_A
Upregulated C_B
Downregulated C_A
Downregulated C_B
Gene Ratio
0.02
0.04
0.06
0.08
0.10
–log (adjusted p-value)
7
6
5
4
B
B/A
C/A
C/B
CSF1R
FGR
TK
PTK2
TKL
BTK
ACVR2A
IRAK4
PBK
STK3
STE
STK24
CMGC
PRAG1
PIK3R4
CK1
CDK6
CDK19
TBK1
BMP2K
CDK1
NEK5
MYLK
PRKACB
AGC
CAMK
ZAK
WNK1
MLKL
CDC7
TP53RK
VRK1
TTN
AURKA
PRKCD
PRKCA
PRKACB
PRKCB
MKNK1
CAMK2B
TGFBR1
MAP3K2
MINK1
TNIK
MAP2K3
STK38L
Upregulated [≥log2(+1)]
Downregulated [≤log2(-1)]

A

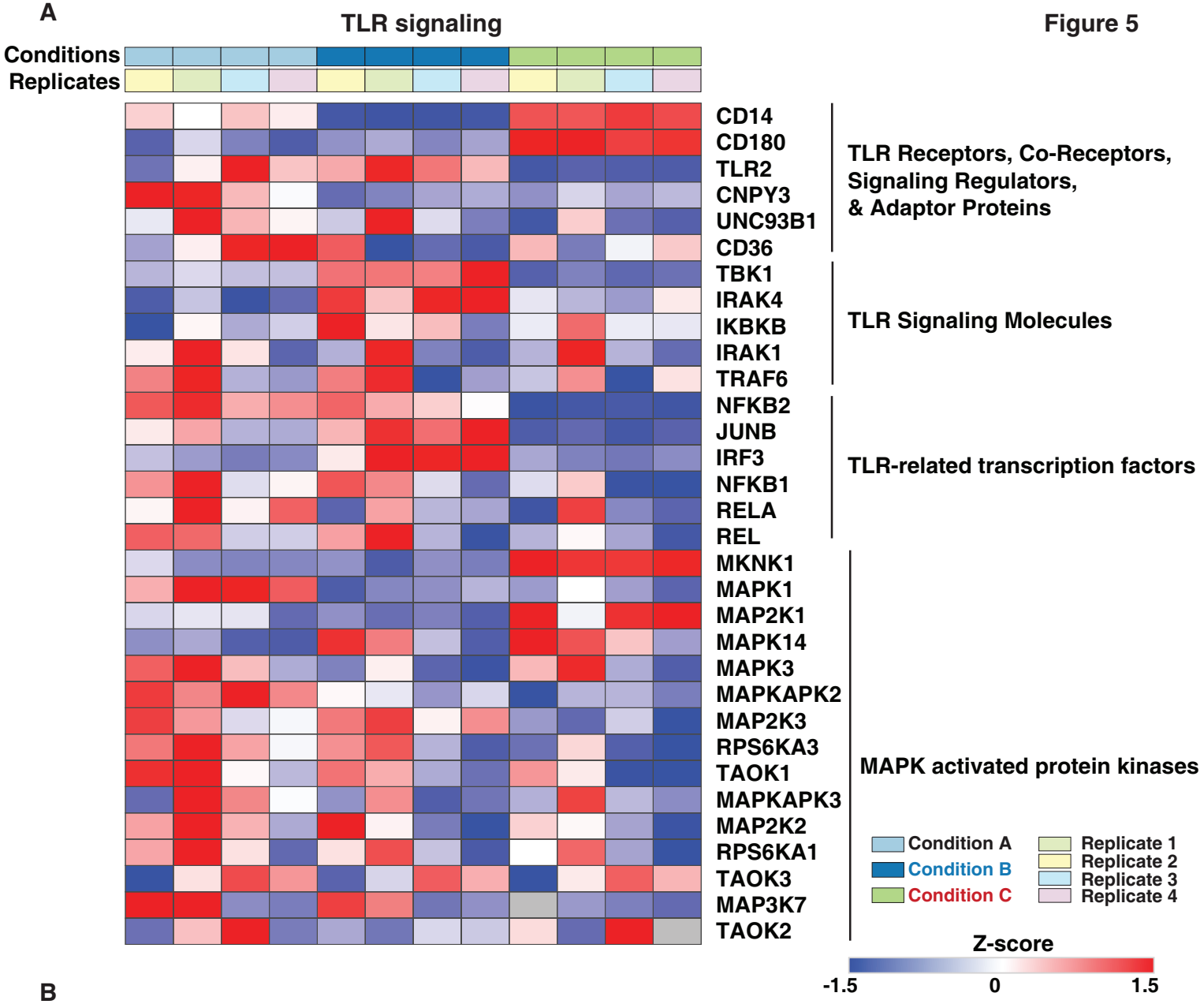
TLR signaling
Conditions
Replicates
CD14
CD180
TLR2
CNPY3
UNC93B1
CD36
TBK1
IRAK4
IKBKB
IRAK1
TRAF6
NFKB2
JUNB
IRF3
NFKB1
RELA
REL
MKNK1
MAPK1
MAP2K1
MAPK14
MAPK3
MAPKAPK2
MAP2K3
RPS6KA3
TAOK1
MAPKAPK3
MAP2K2
RPS6KA1
TAOK3
MAP3K7
TAOK2
TLR Receptors, Co-Receptors, Signaling Regulators, & Adaptor Proteins
TLR Signaling Molecules
TLR-related transcription factors
MAPK activated protein kinases
Condition A
Condition B
Condition C
Replicate 1
Replicate 2
Replicate 3
Replicate 4
Z-score
-1.5
0
1.5

B

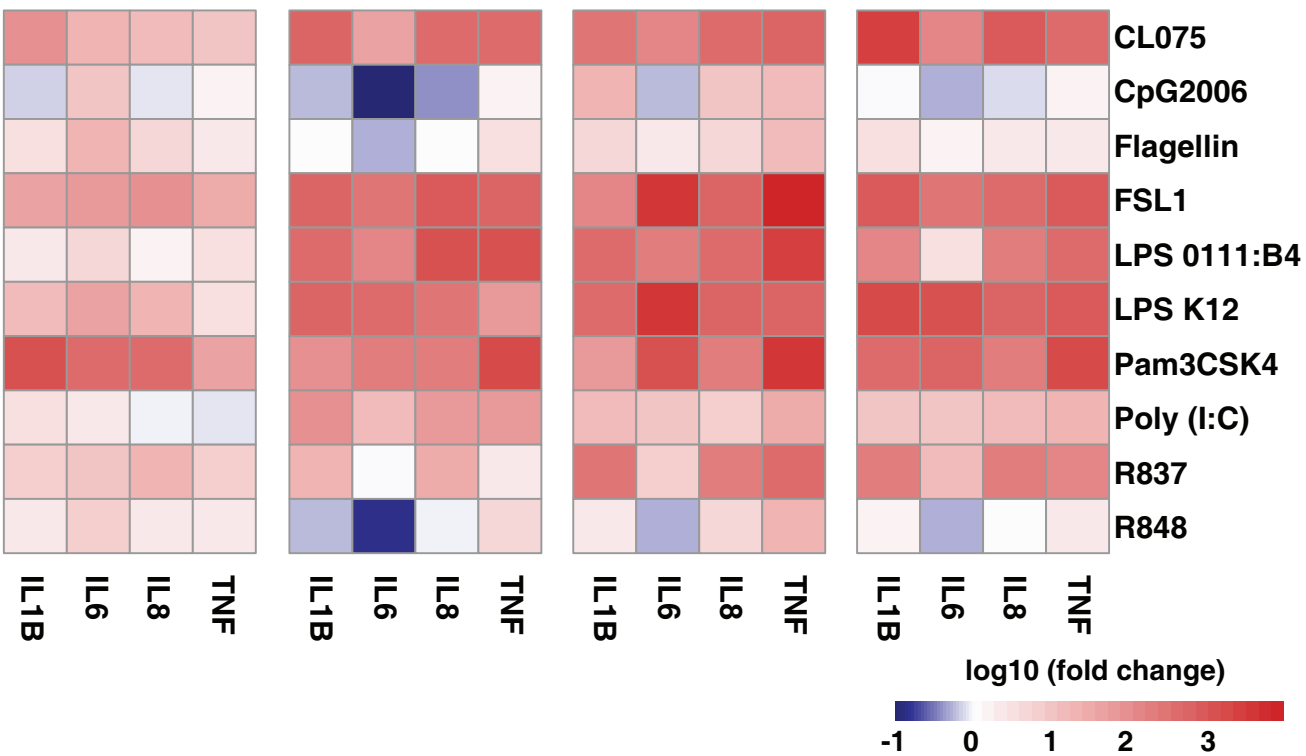
Undifferentiated
Condition A
Condition B
Condition C
CL075
CpG2006
Flagellin
FSL1
LPS 0111:B4
LPS K12
Pam3CSK4
Poly (I:C)
R837
R848
IL1B
IL6
IL8
TNF
log10 (fold change)
-1
0
1
2
3